Band effects on inelastic scattering of low-energy ions from metallic and ionic surfaces: A formalism beyond the adiabatic molecular-orbitals calculation

Evelina A. García
Instituto de Desarrollo Tecnológico para la Industria Química (CONICET-UNL), Güemes 3450, Casilla de Correo 91, 3000 Santa Fe, Argentina

E. C. Goldberg
Instituto de Desarrollo Tecnológico para la Industria Química (CONICET-UNL), Güemes 3450, Casilla de Correo 91, 3000 Santa Fe, Argentina
and Facultad de Bioquímica y Ciencias Biológicas, Universidad Nacional del Littoral, Santa Fe, Argentina
(Received 22 July 1997)

Charge exchange and inelastic excitation processes have been analyzed in the scattering of low-energy He^+ from metallic and ionic surfaces. An Anderson-like Hamiltonian is proposed, where the parameters are defined taking into account the electronic band structure of the surface as well as the atomic nature of the interaction between the projectile and the target atoms. The time-dependent collisional process is solved by using a Green-function formalism, which allows us to calculate not only the charge-state probabilities but also the one-electron interband excitations in the solid. Competitive effects of the hybridizations among the localized state at the projectile site and the localized and extended surface states are contemplated. In this way we can explain the observed energy dependences of the neutralization probability, as well as the occurrence of energy-loss processes due to the excitation of valence and core surface electrons induced by the collision.
[S0163-1829(98)03708-4]

I. INTRODUCTION

The inelastic scattering of low-energy ions from solid surfaces is a typical time-dependent quantum process which is not completely solved at present. It is usual, for visualizing the charge-exchange process, to divide the projectile trajectory into three parts: the incoming trajectory, the violent collision zone, and the outgoing trajectory. Auger neutralization along the incoming part is expected to be important in the case where the ion energy level lies deep enough below the Fermi level. But it is found that the violent collision is crucial for determining the final charge state of the projectile due to the reionization processes, and also for explaining the inelastic channels related with the excitation of target electrons.[1–7] The strong dependence of the inelastic scattering on the ion-target combination suggests that the electronic excitation is closely related to the formation of quasimolecular states during the collision. In this sense a predominance of one-electron over two-electron excitations in surface scattering processes, basically caused by the energy-level crossings,[8] is also justified. The effect of the localized states in the solid (core states) in the scattering process has been analyzed through an ample variety of experimental results.[3–5] It is found that an appreciable ionization of neutral He projectiles at low incident energies ($E_k < 1$ keV) can be expected when there are localized states in the surface with binding energies larger than that of the projectile state. The hybridization among them gives way to antibonding states which favor the electron transfer from the projectile state to the empty band of the solid. In this form it is possible to explain the large reionization probabilities measured in He^+ scattering from alkaline-earth elements,[3] unexpected if one takes into account the deep location of the He-1s energy level with respect to the Fermi level of the solid target. It is the role of ''intermediary agents'' played by the localized states in the surface that allows one to understand the experimental evidence.[9] In the same sense the hybridization between the projectile state and the extended and localized states of the solid provide a mechanism to explain the one-electron excitations in the solid induced by the collisional process. Taking into account the antibonding interaction between the He-1s state and the core levels of the solid, one would expect that these core levels, which promote an important reionization, do not contribute to the inelastic scattering by core-band excitations. A He^+ peak in the scattered ion energy spectra associated with an energy loss around 20 eV can be due to both reionization and core-electron excitation processes, in this case one would think in the active presence of at least two core levels: one with binding energy lower than that for He-1s state (24.6 eV) contributing to the inelastic scattering by core electron excitation, and the other with binding energy larger than 24.6 eV promoting the reionization. The 3p and 3s core states of K resemble this situation.[3]

For a theoretical explanation of both the reionization of He and its electronic excitation, an electron promotion mechanism mediated by molecular orbitals (MO) has been proposed.[2–3,10] On the basis of the adiabatic MO calculation, surface electronic levels can be promoted due to the antibonding interaction, with the projectile orbital promoted in turn by the interaction with a core state of the target atoms. This MO energy calculation cannot give answers either about the reionization and electronic excitation probabilities, or about the dynamical aspects of the hybridizations among the localized state at the ion site and the surface states of localized and extended nature. The first attempt at including

the effect of the hybridizations into a dynamical description was performed by Muda and Newns,[11] by considering, within the framework of the Anderson-Newns Hamiltonian, the projectile-site term as the energy of the diabatic state which results from the interaction between the projectile state and the inner states of the target atom. Solving the time-dependent Schrödinger equation, they found the average occupation number of the projectile state for a linear substrate of a finite number of atoms, with all the interference effects that a dynamical process implies.

By following the ideas of Muda and Newns, our theoretical proposal, which was already presented in previous works,[9,12,13] is an extension of the Anderson-like picture, and include several electronic bands of localized and extended natures, with Hamiltonian parameters assimilated to those obtained from a model based on a superposition of pair bonds,[14,15] which accounts for a realistic description of each dimeric system. Our model calculation conjugates the atomic properties that determine interactions between atoms with a model for the surface states that is capable of reproducing the main features of each projectile-target combination. The time-dependent scattering process is solved using a Green-function formalism which allows us to calculate not only the projectile charge-state probability, but also the probabilities of the one-electron interband excitations induced by the collision, through a very efficient numerical calculation. This formalism also provides probabilities along the projectile trajectory, and the partial contributions of each surface electronic band to the neutralization of the ionic projectile, by resonantlike processes.

The aim of this work is a comparative study of the reionization process and inelastic scattering of low-energy He^+ from metallic and ionic compound surfaces, such as Li, Na, K, LiCl, NaCl, and KI. These selected systems offer an ample variety of features related to the extended band structure and the core states, which makes possible both MO promotion and direct quasiresonant charge-transfer mechanisms. The effect of extended and localized states in the solid, through their competitive hybridizations with the localized state in the ion site, is analyzed in detail.

In Sec. II we describe the interaction Hamiltonian used, and the Green-function formalism for solving the time-dependent collisional process. In Sec. III we present the eigenstates and the eigenenergies which correspond to the linear chain approximation of both metallic and ionic solids. Section IV is devoted to an analysis and discussion of the results, while the conclusions are summarized in Sec. V.

II. THEORY

A. Model interaction Hamiltonian

The projectile-surface interaction is described by an Anderson-like Hamiltonian

$$H(t)=\sum_{\mathbf{k}n}\varepsilon_{\mathbf{k}n}\hat{n}_{\mathbf{k}n}+\sum_{l}\varepsilon_l\hat{n}_l+E_a(t)\hat{n}_a+\sum_{l}[V_{la}(t)\hat{c}_l^{+}\hat{c}_a+V_{al}(t)\hat{c}_a^{+}\hat{c}_l]+\sum_{\mathbf{k}n}(V_{\mathbf{k}n,a}(t)\hat{c}_{\mathbf{k}n}^{+}\hat{c}_a+V_{a,\mathbf{k}n}(t)\hat{c}_a^{+}\hat{c}_{\mathbf{k}n})+V_{n\text{-}n}, \tag{1}$$

where the first two terms are related to the energy states of the solid, the third one to the energy state of the projectile, and the following two to the hopping between solid and projectile states. The screened nuclear repulsion term $V_{n\text{-}n}$ is also included in the expression of $H(t)$ [Eq. (1)]. The $\hat{c}_{\mathbf{k}n}^{+}$, $\hat{c}_l^{+}$ ($\hat{c}_{\mathbf{k}n},\hat{c}_l$) operators create (destroy) an electron in the extended $\varphi_{\mathbf{k}n}$ and localized φ_l states of the solid, respectively. $\hat{c}_a^{+}$ ($\hat{c}_a$) creates (destroys) an electron in the projectile φ_a state. The number operators $\hat{n}_\alpha$ are given by $\hat{n}_\alpha=\hat{c}_\alpha^{+}\hat{c}_\alpha$. The spinless picture is appropriate for the scattering of He^+ (He^0), where it is possible to consider only one active level with binding energy $E_a(\infty)=-24.6$ eV measured with respect to the vacuum level. The extended solid states $\varphi_{\mathbf{k}n}$ with energies $\varepsilon_{\mathbf{k}n}$ (n is the band index) are distinguished from the localized states φ_l with energies ε_l. In the case of localized states associated with core bands, these bands are assumed to be of zero width, and with an energy ε_l equal to the x-ray spectroscopic value.[16,17]

The hopping parameters $V_{\mathbf{k}n,a}(t)$, $V_{la}(t)$, are calculated by performing linear combination of atomic orbitals (LCAO) expansion of the $\varphi_{\mathbf{k}n}$ and φ_l states,

$$V_{\mathbf{k}n,a}(t)=\sum_{\alpha,i}c_{\alpha,i}^{\mathbf{k}n}V_{\alpha i,a}(t), \tag{2a}$$

$$V_{la}(t)=\sum_{\mu,j}c_{\mu,j}^{l}V_{\mu j,a}(t), \tag{2b}$$

where the indexes $\alpha,i(\mu,j)$ denote the site and state of the atoms in the solid, respectively. The expansion coefficients $c_{\alpha,i}^{\mathbf{k}n}$ ($c_{\mu,j}^{l}$) determine the local and partial density of states given by the expression

$$\rho_{\alpha,i}(\varepsilon)=\sum_{\mathbf{k}n}|c_{\alpha,i}^{\mathbf{k}n}|^2\delta(\varepsilon-\varepsilon_{\mathbf{k}n}).$$

The atomic hopping $V_{\alpha i,a}(t)$ between the state φ_a localized in the projectile and the state φ_i localized in the atom site α of the solid is obtained from a self-consistent full electron Hartree-Fock (HF) calculation of the total energy of the corresponding dimer.

The $E_a(t)$ parameter is the projectile energy level shifted by the interaction with the nuclei and electrons of the target within the HF approximation.[14,15] The screened nuclear repulsion $V_{n\text{-}n}$ is calculated within an adiabatic description as the difference between the mean interaction energy and the mean value of the electronic terms retained for describing the dynamical scattering process [Eq. (1)]. This residual interaction identified with $V_{n\text{-}n}$ is well fitted by a Molliere-like potential.

B. Time-dependent formalism

The collisional process is solved by using the time-dependent Green functions defined as follows:

$$G_{q\alpha}(t,t_0)=i\Theta(t-t_0)\langle\psi(t_0)|\hat{c}_\alpha^{+}(t_0)\hat{c}_q(t)+\hat{c}_q(t)\hat{c}_\alpha^{+}(t_0)|\psi(t_0)\rangle, \tag{3}$$

where $\hat{c}_\alpha^{+}(t_0)$ creates an electron in an eigenstate φ_α of the projectile-surface system at the initial time t_0, and $\hat{c}_q(t)$ de-

stroys an electron in an eigenstate φ_q of the noninteracting projectile-surface system at the time value t. In the scattering process both basis sets $\{\varphi_\alpha\}$ and $\{\varphi_q\}$ are coincident, and correspond to the unperturbed solid and projectile states $\{\varphi_{\mathbf{k}n},\varphi_l,\varphi_a\}$.

Within an independent-particle model, it is straightforward to show that the Green function $G_{q\alpha}(t,t_0)$ is proportional to the coefficient $c_q^\alpha(t)$, which gives the weight of the state φ_q in the time-dependent one-electron wave function $\chi_\alpha(t)$ which evolves from the eigenstate φ_α at the initial time t_0:

$$G_{q\alpha}(t,t_0)=i\Theta(t-t_0)c_q^\alpha(t).$$

Therefore, these Green functions provide the information necessary for calculating the probabilities of the different electronic channels we are interested in: the He^+ neutralization probability

$$P^0(t)=\langle\hat{n}_a(t)\rangle=\sum_{\mathbf{k}n<\mathbf{k_F}}|G_{a,\mathbf{k}n}(t,t_0)|^2+\sum_l|G_{al}(t,t_0)|^2; \tag{4}$$

the He^0 ionization probability

$$P^+(t)=1-\langle\hat{n}_a(t)\rangle=\sum_{\mathbf{k}n>\mathbf{k_F}}|G_{a,\mathbf{k}n}(t,t_0)|^2; \tag{5}$$

the excitation probability of one electron from the valence to the conduction band,

$$P_{\mathrm{ve}}(t)=\sum_{\mathbf{k}n>\mathbf{k_F}}\sum_{\mathbf{k}'n'<\mathbf{k_F}}|G_{\mathbf{k}n,\mathbf{k}'n'}(t,t_0)|^2; \tag{6}$$

and the excitation probability of one electron from a localized band to the conduction band,

$$P^e_{\mathrm{lo}}(t)=\sum_{\mathbf{k}n>\mathbf{k_F}}|G_{\mathbf{k}n,l}(t,t_0)|^2. \tag{7}$$

The Green functions $G_{q\alpha}(t,t_0)$ are calculated from their motion equations determined by the Anderson-like Hamiltonian $H(t)$ [Eq. (1)]. After same algebra, and introducing the phase transformation

$$G_{q\alpha}(t,t_0)=g_{q\alpha}(t,t_0)\exp\left[-i\int_{t_0}^t\varepsilon_q(\tau)d\tau\right],$$

the final expressions for the equations of motion are[18]

$$\frac{d}{dt}g_{a\alpha}(t,t_0)=-i\left\{\int_{t_0}^t d\tau\Sigma(t,\tau)g_{a\alpha}(\tau,t_0)+\sum_\beta\widetilde{V}_{a\beta}(t)g_{\beta\alpha}(t_0,t_0)+\delta(t-t_0)\delta_{a\alpha}\right\}, \tag{8a}$$

$$\frac{d}{dt}g_{\mathbf{k}m,\alpha}(t,t_0)=-i\{\widetilde{V}_{\mathbf{k}m,a}(t)g_{a\alpha}(t,t_0)+\delta(t-t_0)\delta_{\mathbf{k}m,\alpha}\}, \tag{8b}$$

$$\frac{d}{dt}g_{l\alpha}(t,t_0)=-i\{\widetilde{V}_{la}(t)g_{a\alpha}(t,t_0)+\delta(t-t_0)\delta_{l\alpha}\}, \tag{8c}$$

where

$$\widetilde{V}_{\beta a}(t)=V_{\beta a}(t)\exp\left[i\int_{t_0}^t[\varepsilon_\beta-E_a(\tau)]d\tau\right],$$

$$\Sigma(t,\tau)=-i\Theta(t-\tau)\sum_\beta\widetilde{V}_{a\beta}(t)\widetilde{V}_{\beta a}(\tau),$$

and the initial condition is given by $g_{q\alpha}(t_0,t_0)=i\delta_{q\alpha}$. The index α runs over the projectile and solid states, while β runs only over the extended and localized states of the solid.

The total-energy conservation is ensured by performing an eikonal approximation of the wave function which describes the coupled motion of nuclei and electrons.[19] A Hamilton-Jacobi equation is derived by taking the classical limit for the nuclei motion,

$$E=\tfrac{1}{2}m\nu^2+V(t),$$

where E is the total energy which is conserved, $\frac{1}{2}m\nu^2$ is the kinetic energy of the projectile, and $V(t)$ is the average potential defined as

$$V(t)=\langle\psi(t_0)|H(t)|\psi(t_0)\rangle, \tag{9}$$

with $\psi(t)$ being the time-dependent electronic state, and $H(t)$ is given by Eq. (1). This potential determines the projectile velocity in a self-consistent way with the electronic transition probabilities. In this approximation we are assuming a sufficient massive target atom as to neglect its recoil.

III. LINEAR CHAIN MODEL FOR THE SOLID TARGET

Tight-binding linear chains of atoms have been widely used for representing the solid targets in the atom-surface collisional process.[20–25] The eigenvalues and eigenfunctions of these one-dimensional systems can be calculated exactly, and taking into account that we are interested in describing the band effects in He^+ scattering experiments involving incident and scattered directions close to the surface normal, the linear model is expected to be adequate.

A. Pure element surface

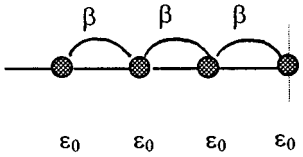

For the semiinfinite linear chain of atoms shown in the figure, with one state per site, the eigenvalues $\varepsilon_{\mathbf{k}n}$ and eigenfunctions φ_k are

$$\varepsilon_{\mathbf{k}n}=\varepsilon_0^{(n)}+2\beta^{(n)}\cos(\pi x), \tag{10a}$$

$$\varphi_{\mathbf{k}}=\sqrt{2}\sum_\alpha\sin(\alpha\pi x), \tag{10b}$$

where

$$x=\lim_{N\to\infty}\frac{\mathbf{k}}{N+1}.$$

TABLE I. Energy parameters that define the band structure, with reference to the vacuum level, for ionic LiCl, NaCl, and KI surfaces (a), and for metallic Li, Na, and K surfaces (b).

(a)

Energy (eV)	LiCl	NaCl	KI
bottom of conduction band	−0.25	−0.30	−0.89
top of valence band	−9.7	−8.5	−7.1
valence-band-width	3.0	3.0	3.0
localized energy state	−19.8 (Cl-3s)	−19.6 (Cl-3s)	−22.4 (K-3p)
	−59.7 (Li-1s)	−40.0 (Na-2p)	−35.0 (K-3s)

(b)

Energy (eV)	Li	Na	K
top of valence band	−2.4	−2.4	−2.2
valence-band-width	3.0	3.0	3.0
localized energy state	−57.0 (Li-1s)	−33.0 (Na-2p)	−20.0 (K-3p)
			−36.1 (K-3s)

Then x varies continuously between 0 and 1. In the case of more than one state per site, nonhybridized bands are considered for each one. The hopping parameter β is obtained from calculations of the partial density of states,[26] and ε_0 is the Fermi level measured with respect to the vacuum level. The energy location of the core bands is obtained from spectroscopic data.[16,17]

B. Ionic compound A-B surface

In this case the linear chain of A-B atoms is represented as follows:

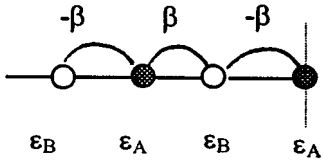

The eigenvalues $\varepsilon_{\mathbf{k}n}$ corresponding to the two bands ($n=1$ and 2) are

$$\varepsilon_{\mathbf{k}n}=\overline{\alpha}+\beta X \tag{10c}$$

with $X=\pm\sqrt{z_1^2+4\sin^2(\pi x/2)}$, $z_1=(\varepsilon_A-\varepsilon_B)/2\beta$ and $\overline{\alpha}=(\varepsilon_A+\varepsilon_B)/2$. The $-$ sign corresponds to the lower and occupied band ($n=1$) and the $+$ sign to the upper and empty band ($n=2$). The gap energy is given by $E_g=|\varepsilon_A-\varepsilon_B|$, and the eigenfunctions $\varphi_{\mathbf{k}n}$ are[18]

$$\varphi_{\mathbf{k}n}=\sum_{\alpha(\text{odd})} c_\alpha^{\mathbf{k}n}\varphi_\alpha+\sum_{\alpha(\text{even})} c_\alpha^{\mathbf{k}n}\varphi_\alpha,$$

with

$$c_\alpha^{\mathbf{k}n}=B\,\sin\left(\frac{\pi x}{2}\right)\left[\frac{2\cos(\alpha\pi x/2)}{\cos(\pi x/2)}+\frac{\sin(\alpha\pi x/2)}{\sin(\pi x/2)}\right]\quad(\alpha\ \text{odd}), \tag{10d}$$

$$c_\alpha^{\mathbf{k}n}=B\,\frac{2\sin\left(\frac{\pi x}{2}\right)\cos\left(\frac{\pi x}{2}\right)}{(X+z_1)}\times\left[\frac{2\cos(\alpha\pi x/2)}{\cos(\pi x/2)}+\frac{\sin(\alpha\pi x/2)}{\sin(\pi x/2)}\right]\quad(\alpha\ \text{even}), \tag{10e}$$

where

$$B=\frac{\sqrt{2}|X+z_1|\cos(\pi x/2)}{\sqrt{(X+z_1)^2\cos^2(\pi x/2)[1+4\cos^2(\pi x/2)]+4\sin^2(\pi x/2)}}.$$

The hopping parameter β is obtained from the valence-band-width w and the gap energy E_g as

$$\beta=\frac{1}{2}\sqrt{w(w+E_g)}.$$

The values of w and E_g, and the energies of the core bands, are obtained from spectroscopic data.[16,17]

In Tables I(a) and I(b) it was show the energy parameters that define the band structures for the different target surfaces we analyzed: LiCl, NaCl, and KI [Table I(a)], and Li, Na, and K [Table I(b)].

Within the linear chain description of the solid target, the LCAO expansion of the coupling term $V_{\mathbf{k}n,a}$ is approximated by considering only the interaction with the first atom of the chain,

$$V_{\mathbf{k}n,a}(t)\approx\sum_i c_{1i}^{\mathbf{k}n}V_{1i,a}(t),$$

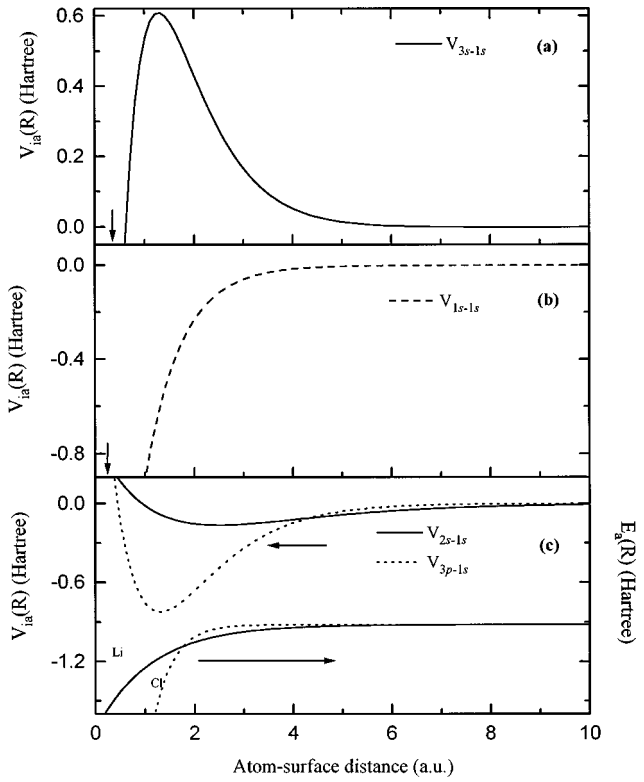

FIG. 1. Hopping parameter obtained from the HF total-energy calculation of the dimer He-target atom as a function of the atom-surface distance. (a) (—) He(1s)-Cl(3s) hopping parameter. (b) (– – – –) He(1s)-Li(1s) hopping parameter. (c) (—) He(1s)-Li(2s) hopping parameter, (----) He(1s)-Cl(3p) hopping parameter, diagonal matrix element $E_a(t)$: (—) for He-Li and (----) for He-Cl.

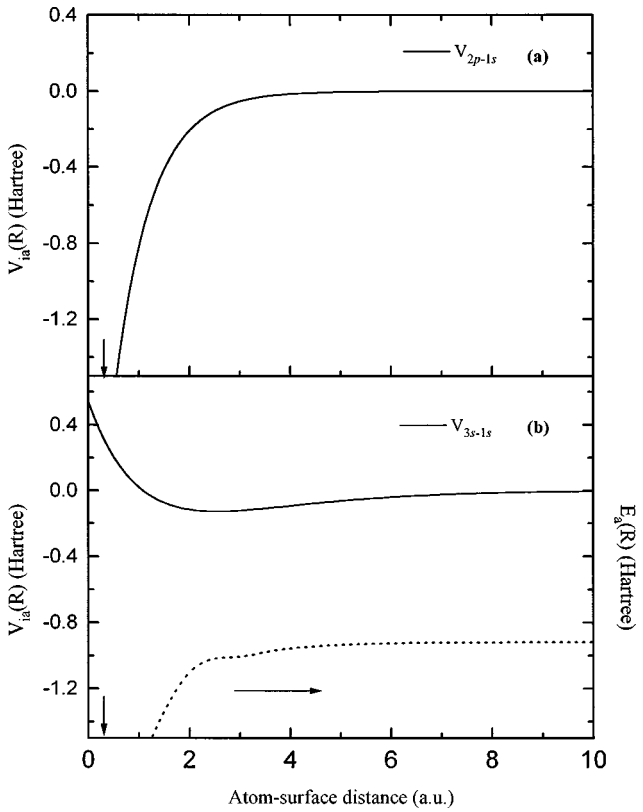

FIG. 2. The same as in Fig. 1: (a) (—) He(1s)-Na(2p) hopping parameter. (b) (—) He(1s)-Na(3s) hopping parameter, (----) diagonal matrix element $E_a(t)$ for He-Na.

where $c_{1i}^{\mathbf{k}n}$ corresponds to $\alpha=1$ in Eq. (10b) for a pure element surface, and in Eq. (10e) for the ionic compound surface. The first atom of the chain is chosen according with the experimental situation we are describing: the scattering of He^+ (He^0) by either the cation or anion.

The projectile trajectory along the chain direction is given by

$$R=R_c(\nu)+\nu(t)t,$$

with both the turning point $R_c(\nu)$ and the velocity determined self-consistently from the average potential $V(t)$ given by Eq. (9).

IV. RESULTS AND DISCUSSION

The atomic hopping $V_{ia}(R)$ parameter and the $E_a(R)$ parameter, obtained from a HF total-energy calculation for each projectile-target combination, are shown in Figs. 1, 2, and 3. The index i runs over the valence and the active core states of the target: $i=2s$ and $1s$ for Li, $i=3s$ and $2p$ for Na, $i=4s$, $3s$, and $3p$ for K, and $i=3p$ and $3s$ for Cl. The HF calculation was performed up to a distance of 1 a.u., the curves fitting these values were extended to smaller distances. The turning point for the maximum value of the kinetic energy considered ($E_{\mathbf{k}}=1000$ eV) is indicated by an arrow in each case.

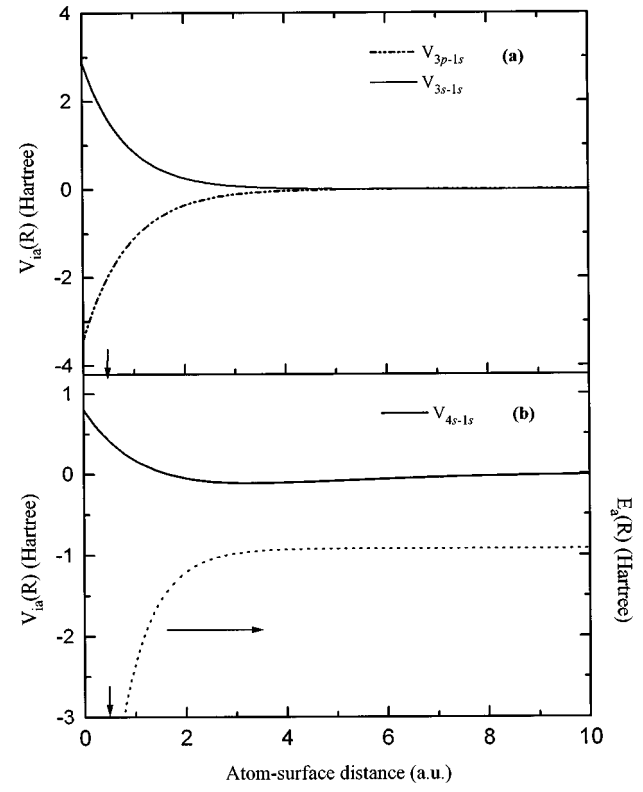

FIG. 3. The same as in Fig. 1: (a) (—) He(1s)-K(3s) and (-·-·-) He(1s)-K(3p) hopping parameters. (b) (—) He(1s)-K(4s) hopping parameter, (---) diagonal matrix element $E_a(t)$ for He-K.

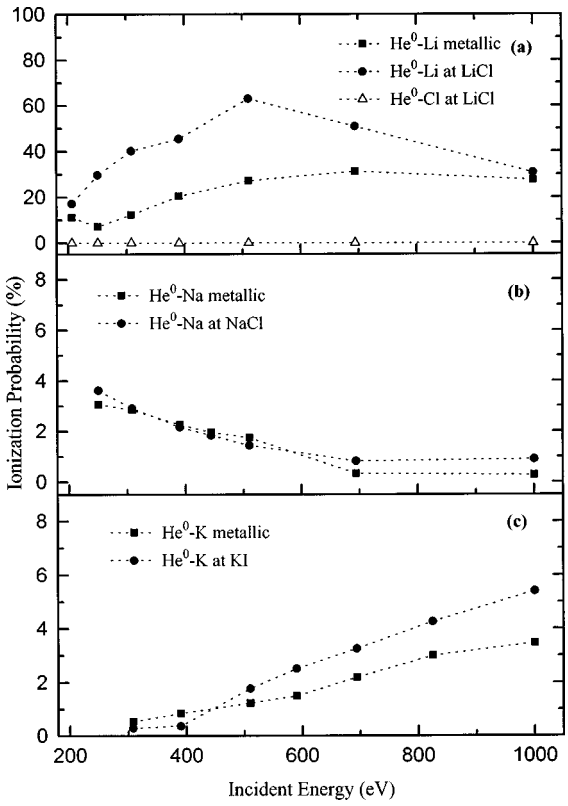

FIG. 4. Ionization probability (%) as a function of projectile kinetic energy of He^0 scattered from metallic and ionic surfaces. (a) He^0 scattered by a Li atom at metallic Li (■) and ionic LiCl (●) surfaces; He^0 scattered by a Cl atom at a LiCl surface (△). (b) He^0 scattered by a Na atom at metallic Na (■) and ionic NaCl (●) surfaces. (c) He^0 scattered by a K atom at metallic (K) (■) and ionic (KI) (●) surfaces.

A. Ionization probability of He^0 scattered by metal and ionic surfaces

The neutral projectile case in our model calculation resembles the reionization experimental situation when the Auger neutralization probability in the incoming trajectory is equal to 1. In other case, our results for the ionization probability of He^0 would be affected by a number less than 1 in order to compare with the observed reionization of He^+.

He^0–Li, LiCl

In Fig. 4(a) we compare the ionization probabilities (P^+) of He^0 scattered from a metallic Li surface, and by Li and Cl atoms at LiCl surface. For the ionic surface, the electron transfer from the He-1s state to the empty-band states is only appreciable when the projectile is scattered by the cation. This is an expected result taking into account that the hybridization between the He-1s (-24.6 eV) and the Li-1s (-59.7 eV) states gives place to an antibonding state which crosses the empty band with a strong weight of He, and that the empty band has a predominant character of Li-2s state.[18,27] While the negligible ionization of He^0 scattered by the Cl atom is consistent with the antibonding interaction with a core state whose binding energy is lower than the one for the projectile state. The behavior of P^+ as a function of the projectile kinetic energy depends on the variation of the antibonding state along the trajectory, on the velocity-dependent turning point, and on the resonance condition with the empty states. The differences between the ionic and metallic surfaces can be adduced to the presence of an energy gap in the first case.

TABLE II. Ionization probability (%) of He^0 scattered by Li atoms at ionic (LiCl) (a) and metallic (b) surfaces. II.1: the interaction between the localized Li-1s core band and the He-1s orbital is considered. II.2: this interaction is omitted in the calculation.

(a)		
E_k (eV)	II.1	II.2
308	40.4	0.1
390	45.5	0.1
510	63.0	0.1
694	51.0	0.1
1000	31.0	0.2
(b)		
E_k (eV)	II.1	II.2
308	12.4	0.1
390	20.5	0.1
510	27.3	0.1
694	31.5	0.1
1000	27.7	0.2

In Table II we compare the P^+ values for the scattering of He^0 from Li atoms at ionic (a) and metallic (b) surfaces with those obtained when the interaction with the localized state of the solid is omitted. These results support clearly the role of ''intermediary agent'' played by the Li-1s state through the hybridization with the He-1s state, in the electron transfer to the band states.

He^0–Na, NaCl

In Fig. 4(b) we present the results of P^+ as a function of the projectile energy when the He^0 is scattered from Na atoms at the metallic surface and at the ionic one. The ionization probabilities are comparable in both ionic and metallic surfaces. The ionization probability is smaller than in the case of He scattered by Li atoms. This fact can be explained in terms of the 2p core-state energy of Na (-33.6 eV for NaCl, -33 eV for metallic Na) which are closer to the He level energy. Then a less promoted antibonding orbital with a smaller weight of He state than in the case of Li results.

In Table III we make the same comparison as in Table II but for the Na-atom case, obtaining the same conclusion: it is the interaction with the localized state 2p which makes possible the charge transfer between the He atom and the surface band states.

He^0–K, KI

Figure 4(c) shows the results of P^+ as a function of the incoming projectile energy for He^+ scattered by K atoms at the metallic and at ionic surfaces. Taking into account only the energy location of the K-3s inner state which is thought as the responsible of the ionization, compared with the energy of the Na-2p inner state, the differences observed between He^0 scattered by either Na or K atoms are not ex-

TABLE III. Ionization probability (%) of He^0 scattered by Na atoms at ionic (NaCl) (a) and metallic (b) surfaces. III.1: the interaction between the localized Na-2p core band and the He-1s orbital is considered. III.2: this interaction is omitted in the calculation.

	(a)	
E_k (eV)	III.1	III.2
444	1.9	0.1
510	1.5	0.1
694	0.8	0.1
1000	0.9	0.1
	(b)	
E_k (eV)	III.1	III.2
444	2.0	0.1
510	1.7	0.1
694	0.3	0.1
1000	0.3	0.1

pected. But we have also to take into account the hopping terms in one and other case (Figs. 2 and 3), and also the fact that in the scattering by a K atom, there are two localized inner bands being able of strong interactions with the He-1s state.

In Table IV(a) we compare the results of P^+ for He^0 scattered by K at ionic surface, with those obtained by omitting in the calculation the interaction either with K-3s or K-3p core states. From the comparison of these results we conclude that, in the absence of a K-3s state, the hybridization with the K-3p state also promotes some reionization. By the other hand, the presence of the K-3p state inhibits the large ionization probability obtained by only considering the interaction of the He-1s state with the K-3s core state. This is a clear example of competitive roles of the hybridizations between the all active localized states. Similar conclusions

TABLE IV. Ionization probability (%) of He^0 scattered by K atoms at the ionic KI surface (a) and at the metallic K surface (b). IV.1: considering the interactions with both localized core bands K-3s and K-3p. IV.2: without considering K-3s. IV.3: without considering K-3p.

	(a)		
E_k (eV)	IV.1	IV.2	IV.3
308	0.3	0.2	29.7
390	0.4	0.4	4.8
510	1.8	0.7	7.0
694	3.3	1.4	17.7
1000	5.4	2.3	25.7
	(b)		
E_k (eV)	IV.1	IV.2	IV.3
308	0.6	0.1	27.2
390	0.8	0.1	22.5
510	1.2	0.1	16.6
694	2.2	0.1	10.9
1000	3.5	0.1	7.1

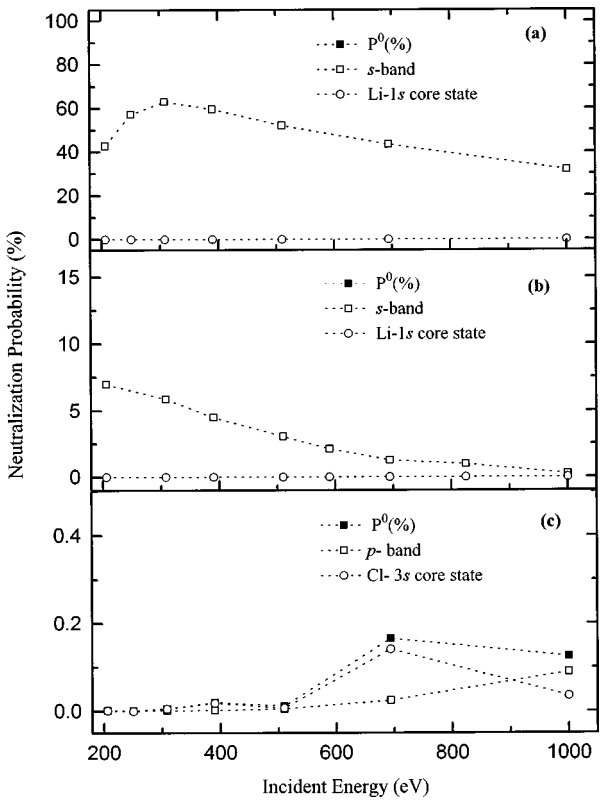

FIG. 5. Neutralization probability (%) as a function of projectile kinetic energy of He^+ scattered from metallic (Li) and ionic (LiCl) surfaces. (a) Partial contributions from 2s band states (□) and from the 1s core state (○) to the total neutralization probability (■) of He^+ scattered by a Li atom at a metallic surface. (b) Partial contributions from 2s band states (□) and from the 1s core state (●) to the total neutralization probability (■) of He^+ scattered by a Li atom at LiCl. (c) Partial contributions from 3p band states (□) and from the 3s core state (○) to the total neutralization (■) of He^+ scattered by a Cl atom at an ionic surface.

are extracted from the results shown in Table IV(b) for He^0 scattered by a K atom at metallic surface. But in this case the interaction with the K-3s state is the only responsible of the ionization mechanism, which is understood by considering the shallower position of the K-3p state in the metallic surface with respect to the ionic one.

The scattering of He^0 by Li, Na, and K atoms at metallic and at ionic surfaces, shows that the ionization probability is strongly dependent on the antibonding interaction between the He-1s orbital and the localized states in the surface. In all cases, the ionization probability we found at the analyzed low-energy values is nearly the same for the scattering from metallic and ionic surfaces. Our results are in agreement with the general trends of the existing experimental data.[3–5]

B. Partial contributions of extended and localized solid states to the neutralization of incoming He^+ projectiles

He^+–Li, LiCl

Figures 5 show the neutralization probability (P^0) of He^+ when it is scattered from Li at metallic [Fig. 5(a)] and ionic [Fig. 5(b)] surfaces, and from Cl at a LiCl surface [Fig. 5(c)]. In these figures we can also observe the partial contributions

TABLE V. Neutralization probability (%) of He^0 scattered by Li atoms at ionic (LiCl) (a) and metallic (b) surfaces. V.1: the interaction between the localized Li-1s core band and the He-1s orbital is considered. V.2: this interaction is omitted in the calculation.

(a)		
E_k (eV)	V.1	V.2
308	5.9	0.2
390	4.5	0.2
510	3.1	0.2
694	1.3	0.2
1000	0.3	0.3
(b)		
E_k (eV)	V.1	V.2
308	63.0	0.1
390	59.6	0.1
510	52.1	0.1
694	43.4	0.1
1000	31.8	0.1

of extended (s and p like), and localized (Li-1s and Cl-3s) bands to the neutralization of He^+.

At the metallic surface there is an important neutralization in the whole energy range analyzed, showing a smooth dependence on energy. It is evident that the charge transfer responsible of the neutralization occurs from valence states [Fig. 5(a)] being negligible the contribution of the core band. But the valence-band electrons neutralizing the incoming ion are only possible due to the promotion of the He-1s state by its hybridization with the localized state in the solid. This fact is corroborated by omitting the interaction with the Li-1s state; in this case P^0 falls to zero (Table V).

At the ionic surface, the neutralization probability of He^+ scattered by the Li atom [Fig. 5(b)] becomes more appreciable for the low-energy values, while is negligible in the all range for the scattering from Cl atom [Fig. 5(c)]. For the scattering by the Li atom it is found a smooth energy dependence related with a total contribution coming from valence-band electrons. The neutralization of He^+ scattered by the Li atom at low kinetic energies is only possible due to to the promotion of the He orbital by the antibonding interaction with the Li core state. The negligible values of P^0 obtained when disregarding this interaction are shown in Tables V. The small neutralization found for the scattering by the anion is in disagreement with the experimental results that show a small ion survival probability at low incoming energies.[3] This can suggest that hybridizations among the solid and projectile states for a linear substrate model differ substantially from those for a real three-dimensional surface. In fact, many experimental findings can only be explained by visualizing the MO formation within a cluster model of the surface, including the first neighbors of the target atom.[7,28,29]

He^+–Na, NaCl

In Figs. 6(a) and 6(b) we show the P^0 results when He^+ is scattered from the Na atom at metallic and ionic (NaCl) surfaces, respectively.

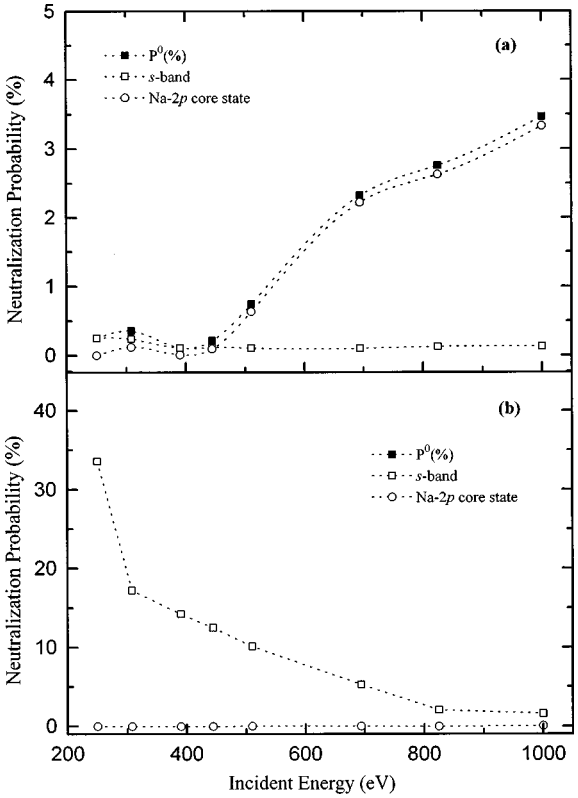

FIG. 6. Neutralization probability (%) as a function of projectile kinetic energy of He^+ scattered from metallic (Na) and ionic (NaCl) surfaces. (a) Partial contributions from 3s band states (□) and from the 2p core state (○) to the total neutralization (■) of He^+ scattered by a Na atom at a metallic surface. (b) The same as in (a) for He^+ scattered by Na atom at ionic surface.

At the metallic surface we observe that for kinetic energies larger than 400 eV the main neutralization mechanism is provided by a nonadiabatic charge exchange between the Na-2p state (−33 eV) and the He-1s state, while, for energies lower than this value, the electron transfer from the valence-band states becomes more important. The mechanism of neutralization for the large energy values is different from the corresponding one for a Li metallic surface. In the Na surface case, the hybridization of the projectile state with the valence-band states appears as the responsible of the quasiresonant charge exchange between the Na-2p and He-1s states.

At ionic surface, for the kinetic-energy range analyzed, the only mechanism possible is a neutralization by the valence-band electrons mediated by the intermediary role of the 2p core state (Tables VI). We observe that the promotion of the He-1s state is more efficient for the neutralization in the case of scattering by Na atoms at a NaCl surface than in the case of scattering by Li atoms at a LiCl surface, while the opposite situation occurs for the ionization of neutral projectiles. This occus with the less-promoted antibonding state in the case of Na lying resonantly with the occupied band states, while, in the Li case, the resonance with the empty-band states is more suitable in the strong interaction region.

He^+–K, KI

A strong contribution to the neutralization of He^+ scattered by a K atom at a metallic surface and at ionic surfaces

TABLE VI. Neutralization probability (%) of He^0 scattered by Na atoms at ionic (NaCl) (a) and metallic (b) surfaces. VI.1: the interaction between the localized Na-$2p$ core band and the He-$1s$ orbital is considered. VI.2: this interaction is omitted in the calculation.

	(a)	
E_k (eV)	VI.1	VI.2
444	12.5	0.3
510	10.2	0.3
694	5.3	0.3
1000	1.6	0.3
	(b)	
E_k (eV)	VI.1	VI.2
444	0.2	0.1
510	0.8	0.1
694	2.3	0.1
1000	3.5	0.1

is provided by a quasiresonant charge transfer from the localized K states to the He-$1s$ state (Fig. 7). The hybridization between them explains the smaller contribution coming from the valence-band states, and also the neutralization at such low energies by the quasiresonant mechanism. The energy dependence of P^0 is in agreement with variations in the incoming energy observed in the elastic peak in the energy spectra of He^+ scattered from K.[4] The appreciable values and the nonmonotonous behavior of the neutralization probability as a function of the incoming ion energy, due to resonant transitions of the surface core electrons to the He state, have been detected in other systems.[30–32] The scattering from Sn (Ref. 30) is an example of target systems where the localized core state (Sn-$4d$ state) is quasiresonant with the projectile orbital. In this case the hybridization between them makes possible a small but appreciable ionization of neutral projectiles with a smooth dependence on the energy, while, for the neutralization of incoming ions, this core state is involved in a direct form through a nonadiabatic charge-transfer process. An oscillatory behavior is obtained for the He^+ neutralization probability due to the direct charge exchange between the localized quasiresonant states. In He^+ scattering from D-covered TiC(111),[31] it has been found that for kinetic energies larger than 40 eV an additional neutralization other than the Auger process takes place. In this case, the mechanism is assumed to be caused by the resonant transition of the D-$1s$ electron to the He state promoted by the antibonding interaction with the Ti-$3p$ core state. In the same sense, the scattering of He^+ by Ta atoms at either pure Ta or TaC surfaces shows a nearly oscillatory energy dependence of the neutralization probability, while, for He^+ scattered by Hf atoms at the HfC surface, the dependence observed is smooth.[32] The Ta-$4f$ core state located at -25 eV (Ref. 17) can be assumed to be responsible for an important resonant neutralization. If the Hf atom has no core states fulfilling such a resonant condition, then the possible mechanism is, in this case, a neutralization caused by a valence-electron transition to the He orbital promoted by interaction with the Hf-$5p$ core state (-30.6 eV).

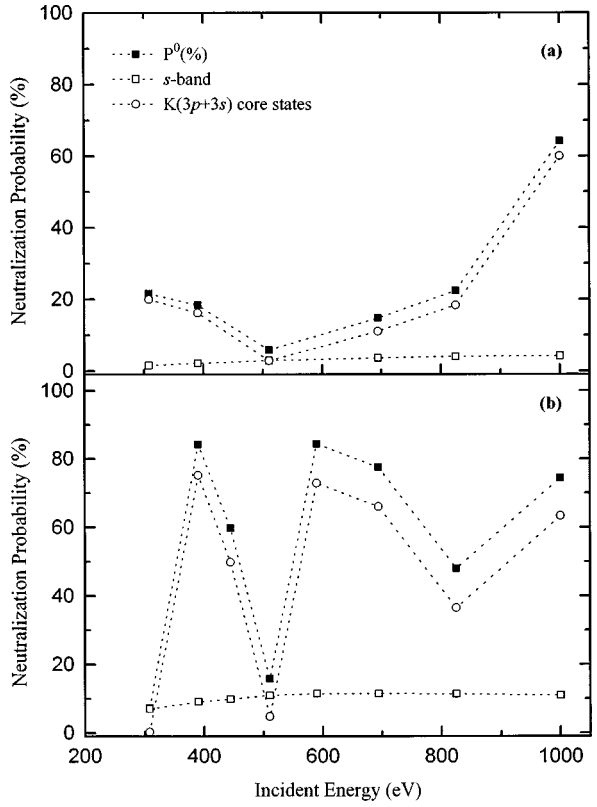

FIG. 7. Neutralization probability (%) as a function of projectile kinetic energy of He^+ scattered by a K atom at metallic (K) and at ionic (KI) surfaces. (a) Partial contributions from $4s$ band states (□), and from $3s$ and $3p$ core states (○) to the total neutralization (■) of He^+ scattered by a K atom at a metallic surface. (b) The same as in (a) for He^+ scattered by a K atom at an ionic surface.

C. Excitation of valence-band electrons

We calculate the excitation probability of valence-band electrons by using expression (6) within our model calculation, that provides one-electron excitations in the solid as well as neutralization of the incoming ion. Then, any attempt to compare our results with the loss peaks associated with interband excitations in the ion energy spectra[2–7,33] would be made taking into account the ion survival probability by Auger and resonant processes. As we are interested in the capability of the ion-surface collision to induce electronic excitations in the solid, we analyze the excitation probabilities independently of the final charge state of the incoming ion.

He^+–Li, LiCl

Figure 8(a) shows the excitation probability of a valence-band electron as a function of the incoming ion energy for He^+ scattered by Li and Cl at a LiCl surface, and by Li at a metallic surface.

At the ionic surface we found that the excitation of a valence-band electron takes place in He^+ scattering by either Li or Cl atoms. We observe that the excitation probability grows with the incoming energy in the case of He colliding with a Cl atom, while it becomes negligible for He^+ scattered by a Li atom. At a metallic surface the excitation probability of valence-band electrons is appreciable in the whole energy range analyzed.

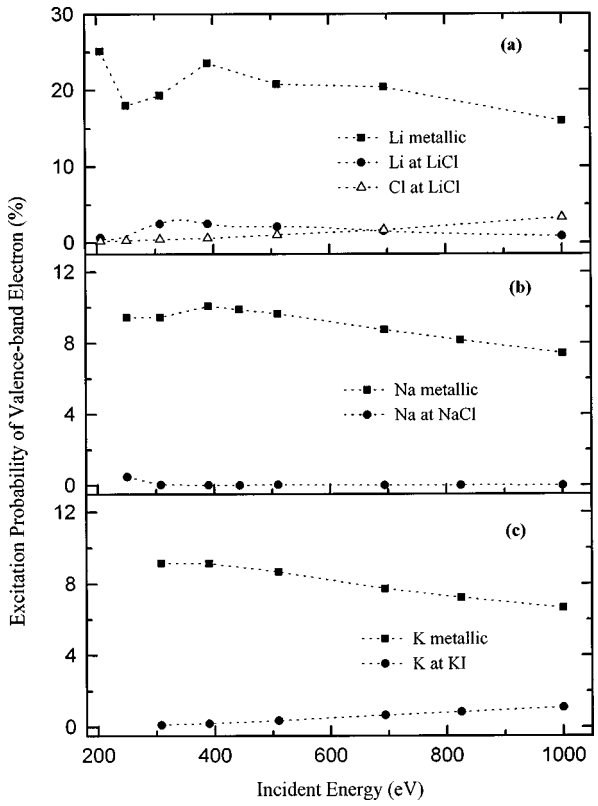

FIG. 8. Excitation probability (%) of valence-band electrons induced by He^+ colliding with metallic and ionic surfaces. (a) He^+ scattered by a Li atom at a metallic surface (■) and at an ionic (LiCl) surface (●); He^+ scattered by a Cl atom at an ionic surface (△). (b) He^+ scattered by a Na atom at a metallic surface (■) and at an ionic (NaCl) surface (●). (c) He^+ scattered by a K atom at a metallic surface (■) and at an ionic (KI) surface (●).

The incidence of localized states in the valence-band electron excitation can be inferred by omitting them in the calculation. In Table VII we compare the results obtained with and without the Li-1s state in the calculation of the valence-band excitation probability when He^+ collides with a Li atom at ionic (a) and metallic (b) surfaces. In the scattering by Li atoms at the ionic surface (a), the interaction with the core state enhances the valence-electron excitation at low kinetic energies, while practically inhibits this excitation at the large energy values analyzed. By suppressing the interaction with the localized state in the metallic surface (b), the excitation probability decreases, and shows a near-constant behavior as a function of the ion energy. This result suggests that the hybridization between the He-1s state and the valence-band states is favored by the antibonding interaction with the Li-1s core state. The energy dependence observed is clearly introduced in this case by variations of the antibonding state along the trajectory.

TABLE VII. Excitation probability (%) of valence-band electrons when He^+ is scattered by a Li atom at an ionic (LiCl) surface (a) and at a metallic surface (b). VII.1: with the Li-1s core band included in the calculation. VII.2: without the Li-1s core band.

	(a)	
E_k (eV)	VII.1	VII.2
308	2.5	0.5
390	2.5	0.9
510	2.2	1.4
694	1.6	2.3
1000	0.9	3.6
	(b)	
E_k (eV)	VII.1	VII.2
308	19.3	
390	23.6	12.6
510	20.8	11.5
694	20.4	10.2
1000	16.0	9.3

TABLE VIII. Excitation probability (%) of valence-band electrons when He^+ is scattered by a Cl atom at an ionic LiCl surface. VIII.1: considering the interaction between the Cl-3s core band and He-1s orbital. VIII.2: this interaction is neglected.

E_k (eV)	VIII.1	VIII.2
250	0.3	0.4
308	0.5	0.6
390	0.6	0.7
510	1.1	1.1
694	1.7	0.9
1000	3.3	1.8

The same comparative analysis is performed in the case of He^+ colliding with a Cl atom at a LiCl surface, the results of which are presented in Table VIII. In this system, hybridizations between the projectile state and the extended and localized states in the solid lead to a competitive effect within the dynamical evolution, and as a consequence the Cl-3s core band partially promotes the valence-electron excitation at the large energy values analyzed.

He^+–Na, NaCl

The interband excitation for He^+ scattered by Na atoms at a NaCl surface is negligible except for very low kinetic energies ($<$300 eV), while it has an appreciable probability in the case of He colliding with Na at the metallic surface, as can be observed from Fig. 8(b). Table IX shows a comparison of the probabilities of valence-band electron excitation obtained with and without the Na-2p core band. In this case, the effect of the core state in the interband excitation is less pronounced than in the Li-surface case. This fact is related to the less efficient promotion of the He-1s state mediated by the interaction with the Na-2p core state, which also leads to a lower ionization of He^0.

He^+–K, KI

An appreciable valence-band electron excitation is found for He^+ colliding with K atoms at the metallic surface, with an energy dependence and probability values similar to those obtained for the case of a metallic Na surface [Fig. 8(b)]. For He^+ scattered at the ionic KI surface, the excitation of valence-band electrons grows with the incoming projectile energy. In Tables X(a) and X(b), we analyze the roles played by the localized K-3s and K-3p core states in the valence-

TABLE IX. Excitation probability (%) of valence-band electrons when He^+ is scattered by a Na atom at an ionic NaCl surface (a), and at a metallic Na surface (b). IX.1: considering the interaction between the Na-2p core band and the He-1s orbital. IX.2: this interaction is neglected.

	(a)	
E_k (eV)	IX.1	IX.2
444	0.02	0.03
510	0.02	0.04
694	0.02	0.08
825	0.02	0.10
1000	0.02	0.24
	(b)	
E_k (eV)	IX.1	IX.2
444	9.9	8.1
510	9.7	7.8
694	8.8	7.0
825	8.2	6.3
1000	7.4	6.3

electron excitation by isolating their effects. We find that the hybridization with the K-3s state produces a marked inhibition of this collisional-induced excitation mechanism at both metallic and ionic surfaces. The K-3p state appears to promote the interband excitation for the large energy values, while for the small energy range we observe a tendency to inhibit this excitation.

Small probabilities of valence-electron excitation are found in He^+ scattering from the ionic surfaces. This excitation process depends on the competitive effects of hybridizations between the projectile orbital and the extended and localized surface states. The absence of an energy gap in the metallic surfaces makes possible a more appreciable valence-electron excitation by the collision.

TABLE X. Excitation probability (%) of valence-band electrons when He^+ is scattered by a K atom at an ionic KI surface (a), and at a metallic K surface (b). X.1: the interactions with both localized core bands K-3s and K-3p, are included. X.2: without the K-3p core band. X.3 without the K-3s core band.

	(a)		
E_k (eV)	X.1	X.2	X.3
308	0.1		3.7
390	0.2		5.0
510	0.4	0.1	5.7
694	0.7	0.2	5.1
1000	1.1	0.2	3.9
	(b)		
E_k (eV)	X.1	X.2	X.3
308	9.2	11.5	24.8
390	9.2	9.3	37.0
510	8.7	7.2	35.6
694	7.7	5.2	31.6
1000	6.7	3.8	26.9

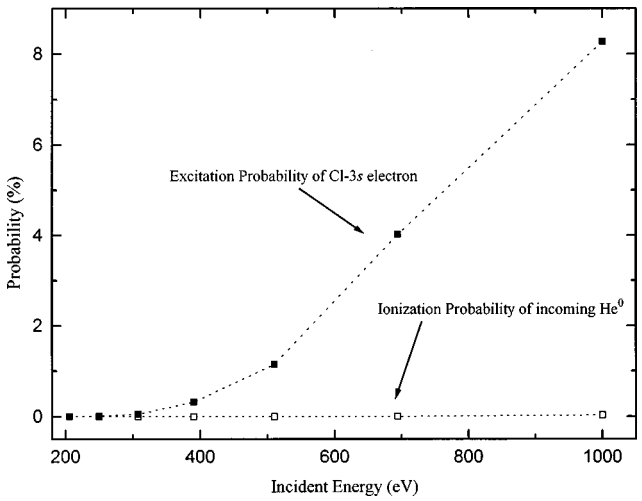

FIG. 9. Core-electron excitation probability (■), and ionization probability of He^0 (□) scattered by a Cl atom at an ionic LiCl surface, both as functions of the incoming projectile energy.

D. Excitation of core-band electrons

In the case of He scattered by Li and Na atoms, it is not found excitation of corelike band electrons (Li-1s and Na-2p). This fact reinforces the antibonding interaction picture between the projectile state and corelike states of the surface. When these corelike states are deeper in energy with respect to the projectile level, the charge exchange between projectile and band states becomes efficient, while the excitation of core electrons is possible when their binding energies are smaller than the ionization energy level of the incoming projectile.

He^+–LiCl

For collision with a Cl atom, one expects a negligible ionization of He^0 due to the quite inefficient antibonding interaction with the Cl-3s core state (-19.8 eV). In terms of the interaction between the localized states, the excitation of the Cl-3s core electron is expected to be appreciable. Our results show these trends, as it can be observed from Fig. 9. The possibility of having a small, but appreciable, core-electron excitation probability for the large kinetic energies shows the simultaneous hybridizations between the He-1s state and the Cl-3p and Cl-3s band states.

He^+–K, KI

The results shown in Fig. 10 indicate the antibonding interaction between the He-1s state and the K-3p core state as the mechanism responsible for this core-electron excitation. We observe that hybridization with the K-3s core state becomes inefficient at low kinetic energies for promoting the excitation of the K-3s electron. Then, these results corroborate the requirement of surface core states with binding energies lower than the one for the projectile state, for-having an appreciable excitation of these core electrons. The different energy dependencies of the K-3p excitation found for the metallic and ionic surfaces are assigned to band-structure effects, fundamentally to the presence of an energy gap in the KI surface. How the simultaneous interactions among

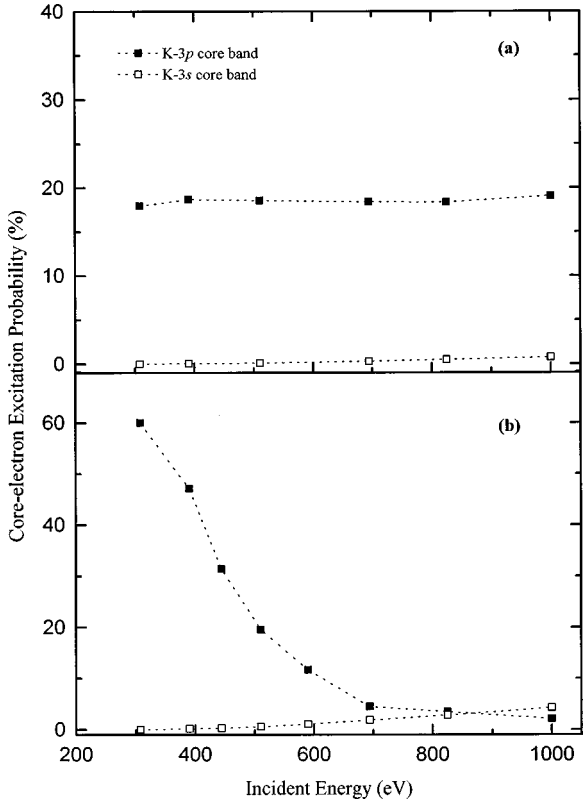

FIG. 10. Energy dependence of the probability of core-electron excitation by the He^+ scattering from K at a metallic surface (a), and at an ionic (KI) surface (b). The excitation probabilities of the K-3p (■) and K-3s (□) core electrons are discriminated.

He-1s, K-3s, and K-3p states is affecting the K-3p core-electron excitation, can be extracted from the results shown in Tables XI(a) and XI(b) by either considering or omitting the interaction with the K-3s state. We observe that in the case of the metallic surface, the hybridization with the K-3s state inhibits the K-3p electron excitation. For the ionic surface case this inhibition effect is also observed for energies larger than 390 eV, but for energy values smaller than this one the interaction with K-3s state potentiates the excitation of the K-3p electron.

Our results show a monotonous increase of the core-electron excitation probability for low kinetic-energy values, in the scattering from KI surface. Assuming a resonant neutralization mechanism as the available one, the oscillatory energy dependence of the loss peak C associated with core-electron excitation[4] can be explained in terms of the calculated P^0 behavior [Fig. 7(b)].

TABLE XI. Excitation probability (%) of the K-3p electron when He^+ is scattered by a K atom at an ionic KI surface (a), and at a metallic K surface (b). XI.1: the interactions with both localized core bands K-3s and K-3p are included. XI.2: the interaction between the K-3s core band and He-1s orbital is omitted.

	(a)	
E_k (eV)	XI.1	XI.2
308	60.0	41.8
390	47.1	63.5
510	19.6	81.2
694	4.6	84.8
1000	2.1	78.0
	(b)	
E_k (eV)	XI.1	XI.2
308	17.9	43.3
390	18.7	30.5
510	18.6	32.5
694	18.4	33.1
1000	19.1	33.5

V. CONCLUSIONS

The theoretical proposal we use in this work to describe the collision between ions and surfaces allows us to analyze in detail the charge exchange and interband excitations due to the one-electron processes. The dynamical aspects of the collision are taken into account, and the effects of the different interactions among the projectile state and the localized and extended surface states are isolated. In this way, we are able to infer the roles played by each one in the charge-exchange and excitation processes. The general trends we obtain for neutralization and reionization of He^0 scattered from either metallic or ionic surfaces, as well as for valence- and core-electron excitations induced by the collision, are in agreement with the experimental findings. The strong dependence on the hybridizations among the projectile state and the surface states leads to results very dependent on the projectile-target combination. This fact also suggests that a suitable description of the surface involving the first neighbors of the target atom can be required for a good description of the quasimolecular state formation.

ACKNOWLEDGMENTS

This work was supported by Grants (PID) No. 3748/92 from Consejo Nacional de Investigaciones Científicas y Tecnológicas (CONICET) and (CAID) No. 94-000-000E12 from Universidad Nacional del Litoral (UNL).

[1] R. Souda and M. Aono, Nucl. Instrum. Methods Phys. Res. B **15**, 114 (1986).
[2] R. Souda, T. Aizawa, C. Oshima, and Y. Ishizawa, Phys. Rev. Lett. **61**, 2705 (1988).
[3] R. Souda, T. Aizawa, C. Oshima, S. Otani, and Y. Ishizawa, Phys. Rev. B **40**, 4119 (1989).
[4] R. Souda, T. Aizawa, C. Oshima, and Y. Ishizawa, Nucl. Instrum. Methods Phys. Res. B **45**, 369 (1990).
[5] R. Souda, T. Aizawa, C. Oshima, and Y. Ishizawa, Nucl. Instrum. Methods Phys. Res. B **45**, 364 (1990).
[6] R. Souda, T. Aizawa, W. Hayami, S. Otani, and Y. Ishizawa, Phys. Rev. B **42**, 7761 (1990).
[7] R. Souda, K. Yamamoto, W. Hayami, T. Aizawa, and Y. Ishizawa, Phys. Rev. B **51**, 4463 (1995).

[8] S. Tsuneyuki and M. Tsukada, Phys. Rev. B **34**, 5758 (1986).
[9] Evelina A. García, P. G. Bolcatto, and E. C. Goldberg, Phys. Rev. B **52**, 52 (1995).
[10] R. Souda, K. Yamamoto, W. Hayami, T. Aizawa, and Y. Ishizawa, Phys. Rev. Lett. **75**, 3552 (1995).
[11] Y. Muda and D. M. Newns, Phys. Rev. B **37**, 7048 (1988).
[12] Evelina A. García, E. C. Goldberg, and M. C. G. Passeggi, Surf. Sci. **325**, 311 (1995).
[13] Evelina A. García and E. C. Goldberg, Surf. Sci. **364**, 193 (1996).
[14] P. G. Bolcatto, E. C. Goldberg, and M. C. G. Passeggi, J. Phys.: Condens. Matter **5**, A105 (1993).
[15] P. G. Bolcatto, E. C. Goldberg, and M. C. G. Passeggi, Phys. Rev. A **50**, 4643 (1994).
[16] *Photoemission in Solids I*, edited by M. Cardona and L. Ley, Topics in Applied Physics, Vol. 26 (Springer-Verlag, New York, 1978); *Band Structure Spectroscopy of Metals and Alloys*, edited by D. J. Fabian and L. M. Watson (Academic, London, 1973).
[17] J. A. Bearden and A. F. Bun, Rev. Mod. Phys. **39**, 125 (1967).
[18] Evelina A. García, Ph.D. thesis, Facultad de Ciencias Exactas, Ingeniería y Agrimensura, Universidad Nacional de Rosario, Argentina, 1997.
[19] E. E. Nikitin and S. Ya. Umanski, in *Theory of Slow Atomic Collisions*, Springer Series in Chemical Physics Vol. 30 (Springer-Verlag, Berlín, 1984); E. C. Goldberg, J. Ferrón, and M. C. G. Passeggi, Phys. Rev. B **40**, 8666 (1989); S. Sawada, A. Nitzan, and H. Metiu, Phys. Rev. B **32**, 851 (1985).
[20] R. Brako and D. M. Newns, Surf. Sci. **108**, 253 (1981).
[21] Y. Muda and D. M. Newns, Phys. Rev. B **37**, 70 489 (1989).
[22] W. Bloss and D. Hone, Surf. Sci. **72**, 277 (1978).
[23] Y. Muda and T. Hanawa, Surf. Sci. **97**, 283 (1990).
[24] K. L. Sebastian, V. C. Jyothi Bhasu, and T. B. Grimley, Surf. Sci. **110**, L571 (1981).
[25] H. K. McDowell, J. Chem. Phys. **77(6)**, 3263 (1982).
[26] D. A. Papaconstantopoulus, in *Handbook of the Band Structure of Elemental Solids* (Plenum, New York, 1986).
[27] R. Hoffmann, Rev. Mod. Phys. **60**, 601 (1988).
[28] R. Souda, K. Yamamoto, B. Tilley, W. Hayami, T. Aizawa, and Y. Ishizawa, Phys. Rev. B **50**, 18 489 (1994).
[29] R. Souda, K. Yamamoto, W. Hayami, B. Tilley, T. Aizawa, and Y. Ishizawa, Surf. Sci. **324**, L349 (1995).
[30] R. Souda, T. Aizawa, C. Oshima, M. Aono, S. Tsuneyuki, and M. Tsukada, Surf. Sci. **187**, L592 (1987).
[31] R. Souda, T. Aizawa, C. Oshima, S. Otani, and Y. Ishizawa, Phys. Rev. B **41**, 803 (1990).
[32] R. Souda, T. Aizawa, S. Otani, and Y. Ishizawa, Surf. Sci. **232**, 219 (1990).
[33] R. Souda, K. Yamamoto, W. Hayami, T. Aizawa, and Y. Ishizawa, Phys. Rev. B **50**, 4733 (1994).